AIP | The Journal of Chemical Physics

Intracavity laser excitation of NCO fluorescence in an atmospheric pressure flame

William R. Anderson, John A. Vanderhoff, Anthony J. Kotlar, Mark A. Dewilde, and Richard A. Beyer

Citation: The Journal of Chemical Physics **77**, 1677 (1982); doi: 10.1063/1.444063
View online: http://dx.doi.org/10.1063/1.444063
View Table of Contents: http://scitation.aip.org/content/aip/journal/jcp/77/4?ver=pdfcov
Published by the AIP Publishing

Intracavity laser excitation of NCO fluorescence in an atmospheric pressure flame

William R. Anderson,[a] John A. Vanderhoff, Anthony J. Kotlar, Mark A. Dewilde, and Richard A. Beyer

U.S. Army Ballistic Research Laboratory, Aberdeen Proving Ground, Maryland 21005

(Received 29 March 1982; accepted 13 May 1982)

Laser excited fluorescence of the NCO radical has been obtained using discrete prism selected lines of an argon ion laser pump source. To our knowledge this is the first time NCO fluorescence has been obtained in a flame environment. NCO was formed in a slightly rich atmospheric pressure CH_4/N_2O flame. This flame was placed inside the extended cavity of the argon laser to take advantage of the much higher light intensity levels. All of the available laser lines pump vibrational hot bands of the NCO $A\ ^2\Sigma^+ \leftarrow X\ ^2\Pi$ system. The 4658 Å line appears to be the most useful for probing NCO densities. This line pumps in the $A\ ^2\Sigma^+(0,0^0,0) \leftarrow X\ ^2\Pi\ (1,0^1,0)$ vibrational band. NCO is pumped to $N' = 31$ by this line, probably via the $Q_2 31$ transition although the $R_2 30$ and $P_2 32$ transitions could not be ruled out in the present analysis. The 4658 Å line was used to determine a relative NCO density profile through the reaction zone of a CH_4/N_2O flame. Profiles of C_2, CN, and temperature were also obtained in this flame and are compared with the NCO profile. A lower limit of approximately 3×10^{14} cm^{-3} was placed on the peak NCO density in the flame. Attempts to find NCO or CN fluorescence in a CH_4/air flame failed indicating probable differences in nitrogen chemistry for the two flames.

I. INTRODUCTION

The NCO radical is thought to play an important intermediate role in hydrocarbon flames, even though it has not been previously observed in a flame environment. In particular, it is postulated that NCO is an intermediate in the conversion of fuel-bound nitrogen to NO_x and N_2 in rich combustion and in production of NO_x in hydrocarbon/air flames.[1] Our interest in NCO results from its possible importance in gun propellant flames. Experimental thermal decomposition studies of various gun propellants show that large quantities of HCHO, HCN, N_2O, and NO_2 are produced.[2] Thus, flames composed of these fuels and oxidizers are of interest. Shock tube studies[3] of the $HCN + NO_2$ system lead to the conclusion that an important pathway for the reaction involves NCO. For these reasons it is of interest to develop a sensitive technique for detection of NCO *in situ* in reactive systems.

NCO is the subject of several previous and contemporary spectral investigations. The A–X system was first identified in low resolution emission spectra upon photolysis of C_2H_5NCO by Holland *et al.*[4] Subsequently, rotational analyses of the absorption spectra have been performed for the A–X system by Dixon[5] and by Bolman *et al.*[6] and for the $B\,^2\Pi$–$X\,^2\Pi$ system by Dixon.[7] NCO A–X system emission, in addition to that from other species, has been used by Okabe[8] to study photolysis of HNCO. In addition to these early gas phase experiments, NCO has been studied in matrix isolation experiments. Milligan and Jacox[9] used this approach to investigate the infrared and ultraviolet absorption spectra. Bondybey and English[10] similarly studied the laser excited fluorescence (LEF) spectra. More recently, in a paper mainly concerning a different subject, Reisler *et al.*[11] reported gas phase radiative lifetimes of several vibrational levels of the A state. Finally, in a study not yet completed, Sullivan *et al.*[12] have detected LEF for both the A and B states of NCO in a flow system. Preliminary measurements include A and B state lifetimes, collisional quenching rates for several added species, and ground vibrational state frequencies.

Recently, spontaneous Raman spectroscopy has been used to probe temperature and species profiles in premixed laminar CH_4/N_2O flames.[13] During the course of these experiments intense laser fluorescences resulting from excitation with various prism selected lines of the probe argon ion laser were discovered. The radical species producing these fluorescences have been identified as C_2, CN, and NCO.[14–17] Measurements involving C_2 and CN[15] concentrations and CN $B\,^2\Sigma^+$ energy transfer[16] in the flame are discussed in separate papers. This paper addresses the spectral identification and concentration profile of NCO in the flame. The present work includes a more detailed description of the apparatus and discussion of the results than appeared previously.[17] Two major issues are addressed. First, the best argon laser line for probing NCO densities and the transition it pumps are discussed. Then an accurate relative density profile is presented along with an estimate of the absolute peak NCO density for our flame conditions. The estimate, which is thought to be good to about a factor of 5, places a lower bound on the NCO density of $\sim 3\times10^{14}$ cm^{-3} in our slightly rich flame.[18] This density is sufficiently large that possible participation of NCO in the flame chemistry should be considered.

II. EXPERIMENTAL

A. Burner

Rich premixed flames of methane and nitrous oxide burning at atmospheric pressure have been studied using an open channel curved knife edge burner shown in Figs. 1 and 2. The burner was recently designed in

[a] Author to whom correspondence should be addressed.

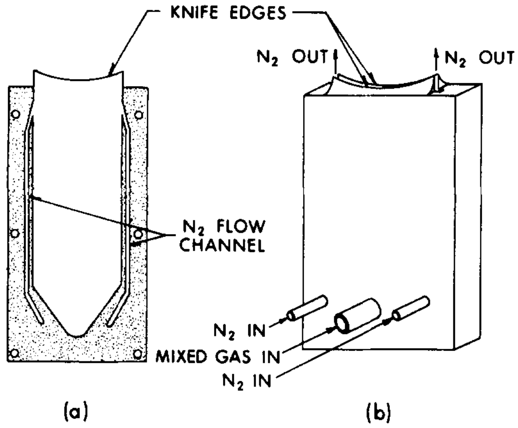

FIG. 1. Diagram of burner used for laser probing of flames. (a) Lengthwise cross section of burner showing large central channel for premixed gases and small N_2 flow channels. (b) Outside view of burner.

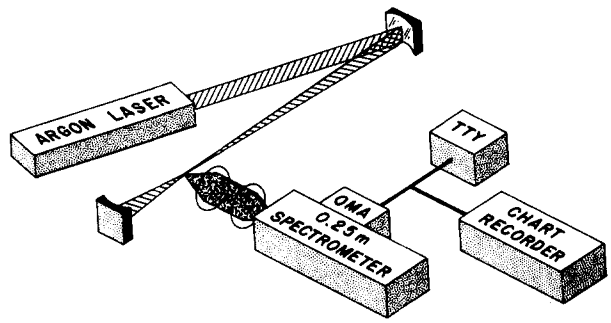

FIG. 3. Optical and electronic apparatus. Two concave mirrors were used to extend the cavity of an argon ion laser. A flame (not shown) was placed at the intracavity focal point. Scattered radiation was focussed onto the slits of a 0.25 m monochromator with OMA detector. Output from the OMA was viewed on a recorder. Hard copy was obtained on a teletype.

this laboratory for intracavity laser probing through the reaction zone of premixed flames.[19] The burner was made from two aluminum plates with various gaskets providing the desired channel width. For these experiments the rectangular channel dimensions were 50 by 3 mm. Two small independent channels run along each side of the main channel and a flow of N_2 through these channels prevents the flame from wrapping around the ends of the knife edges. The burner produces a curved flame front which follows the radius of curvature of the knife edges (50.8 mm). In typical usage a laser beam passes between the knife edges parallel to the top of the burner [Fig. 1(b)]. The cross section in Fig. 2 shows a typical laser beam position. For the present experiments, only a length of about 3 mm of the laser beam was viewed by the detection optics. Since the radius of curvature of the knife edges is much larger than this,

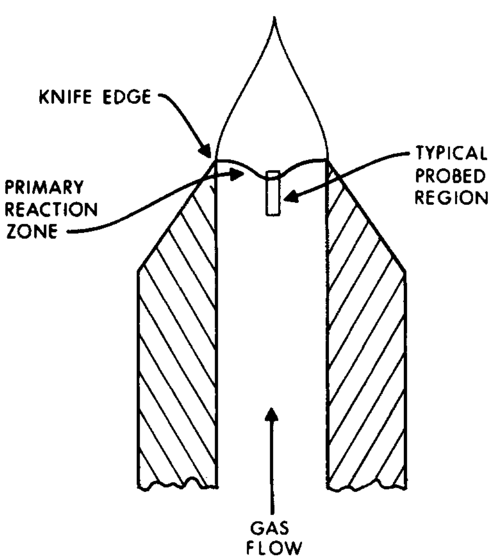

FIG. 2. Cross section across width of burner. A typical flame position is shown. The laser beam is circular in cross section. The rectangular area labeled "typical probed region" was mapped out by moving the burner back and forth through the laser beam.

the results may be treated using one-dimensional flame approximations. The curvature is used to minimize index of refraction effects on the laser beam.

Gas flow to the burner is regulated by rotameters. The fuel oxidizer mixture is expressed as an equivalence ratio ϕ, where ϕ is defined as the actual fuel-oxidizer concentration ratio divided by the stoichiometric fuel-oxidizer concentration ratio (i.e., $4\,[CH_4]/[N_2O]$). The spectroscopic results for NCO were obtained at different times without an emphasis being placed on the exact flame conditions. Here the approximate conditions were $\phi = 1.6$ with 40% dilution by mole fraction with N_2. For the case where the concentration and temperature profiles and the absolute density estimates were obtained, the flow conditions were carefully measured with a wet test meter. The results were $\phi = 1.36 \pm 0.02$ with 45% dilution with N_2. The overall premixed gas flow rate was 1.72 ± 0.05 ℓ/min at 298 K and 1 atm.

Temperature measurements performed on this burner using spontaneous Raman spectroscopy indicate that heat losses to the burner are very small.[19] That is, within experimental error (< 50 K) the maximum flame temperatures measured are the same as obtained from an equilibrium flame temperature calculation assuming adiabatic conditions.

B. Optics and electronics

The experimental arrangement for this study is shown in Fig. 3. A nominal 4 W (all lines) argon ion laser with prism line selection was used as the excitation source. Its cavity was extended with two highly reflective mirrors of focal length 1 and 0.3 m providing an intracavity beam waist of about 100 μm. The intracavity circulating power was about 50 W on the strongest lines. Only minor attenuation occurred when a steady CH_4/N_2O flame was inserted in the cavity at the beam waist. The burner was placed on its side with the open channel facing the detection optics. The burner was attached to a small milling table providing movement in two directions. For the flame profiles measured in the present work the burner motion was along the line of sight of the

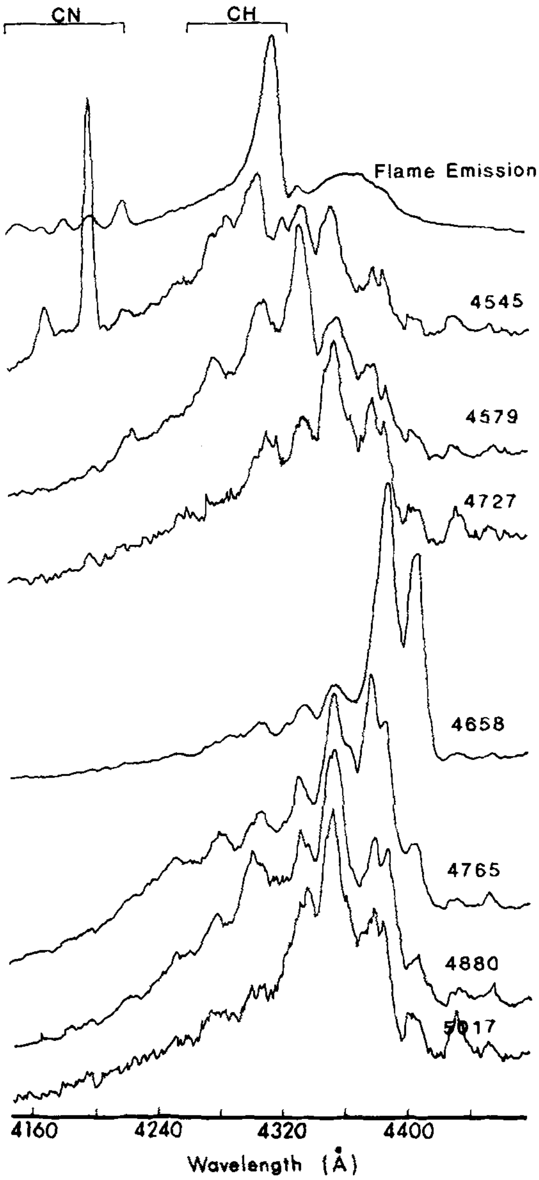

FIG. 4. Flame emission and LEF spectra from a slightly rich CH_4/N_2O flame where the resolution was 3 Å FWHM. The spectra have been normalized so that no information about relative intensities of LEF from the various argon pump lines may be obtained from the figure. The top trace is the flame emission. The other seven traces are LEF spectra resulting from the argon laser pump lines indicated to the right.

detection optics. This motion was monitored using a precision dial gauge which reads directly to 0.01 mm.

For coarse spectral resolution (see Fig. 3) two quartz lenses were used to image a portion of the scattered light onto the 100 μm horizontal slits of a 0.25 m spectrometer mounted on its side. The sampled light came from a volume approximated by a cylinder of 100 μm diameter and 3 mm in length. An optical multichannel analyzer (OMA) with a silicon intensified vidicon tube was used to detect the dispersed light. Using a grating of 1180 grooves/mm, approximately 400 Å of the spectrum could be observed at one time with this system. The radiation was accumulated into 500 channels which, when coupled with the 100 μm entrance slits of the spectrometer, provided a resolution, FWHM, of approximately 3 Å. The data were accumulated for equal lengths of time into the two separate OMA memories first with laser on and then with laser off conditions. The latter provided a flame background emission spectrum. Differencing of these two memories yielded the LEF or Raman spectrum. Accumulation times for data reported here were usually less than 10 s for LEF and about 30 s for Raman scattering data. Frequently, neutral density filters had to be placed in front of the entrance slits of the monochromator to keep the real time LEF signal within the dynamic range of the OMA. Either LEF or Raman signals from the reaction zone of the flame could be readily observed in real time on a display oscilloscope. Our discovery of these unexpected fluorescences may be directly traced to this capability.

While the 0.25 m spectrometer–OMA detection system had sufficient resolution to allow identification of C_2 and CN,[14,15] the rotational structure of NCO was much too dense to allow a firm assignment of the spectrum. For this reason a higher resolution detection system was necessary. Here a 1 m monochromator with a cooled EMI type 9789 QA photomultiplier tube (PMT) wired for photon counting replaced the 0.25 m monochromator–OMA system in Fig. 3. A chopper operating at 40 Hz was placed inside the laser cavity to provide laser on and laser off conditions necessary for the elimination of the background signal. A glass dove prism was placed in front of the entrance slits to rotate the image 90°. The highest resolution achieved with this system was 0.17 Å FWHM. Amplified pulses from the photomultiplier tube were passed through a single channel analyzer which discriminated against noise sources. The output of the single channel analyzer then passed through, in parallel, two linear gates and two rate meters. The flame background was removed from the LEF signal by gating the signal to the two rate meters in synch with the chopper and subtracting the rate meter outputs. The response time of the rate meters was such that these signals appeared continuous and could thus be subtracted easily. The resultant LEF (difference) and flame emission signals were recorded with a dual strip chart recorder. In addition, the separate rate meter outputs could be digitized and stored in a PDP 11/34 computer for later analysis.

III. RESULTS AND DISCUSSION

A. Interpretation of spectral features

As mentioned in the introduction the LEF spectra of NCO were first observed while measuring temperature and major species profiles in a flame using spontaneous Raman spectroscopy. Some typical OMA spectra from this early work[14] are shown in Fig. 4. The upper trace is a flame emission spectrum obtained with the laser blocked. Most of the emission observed is from the $\Delta v = -1$ sequence of the CN $B\,^2\Pi - X\,^2\Sigma^+$ violet system (4140–4220 Å) or from the $\Delta v = 0$ sequence of the CH $A\,^2\Delta - X\,^2\Pi$ system (4240–4400 Å). Higher resolution scans, shown later, indicate that a small fraction of the emission in the CH P-branch region is due to NCO. Fluorescence spectra obtained by subtracting this emission spectrum from the fluorescence plus emission spectra are shown for seven discrete Ar^+ laser pump lines. These individual spectra were normalized and are thus not of similar intensity as depicted in Fig. 4.

Inspection of the fluorescence spectra of Fig. 4 reveals several interesting features. First, one of the laser lines, 4545 Å, pumps CN. Fluorescence from the R and P branches of the (1, 2) band in the B–X system results in the two sharp peaks between 4160 and 4200 Å. Studies described in detail elsewhere[15] showed that the 4545 Å line pumps a (1, 3) $R20$ transition of CN. Second, apart from the CN band, all of the fluorescence spectra consist of a system of bands in an envelope extending from about 4160–4440 Å. Similar appearing band envelopes are also obtained when pumping with the 4965 and 5145 Å lines (not shown). These spectra look similar to the NCO emission spectra observed by Okabe[8] upon photolyzing HNCO. It was for this reason that we originally, tentatively, assigned the spectra to NCO.[14]

The fluorescence spectrum from the 4658 Å pump line was initially selected for detailed examination using the 1 m monochromator for two reasons. First, the shape of the envelope for the banded system is quite different and appears narrower than that from the other pump lines (see Fig. 4). Second, the integrated fluorescence intensity (unnormalized for laser power) is the strongest for the 4658 Å pump line in spite of the fact that this is one of the weakest laser lines. This intense fluorescence may be understood by examining earlier fluorescence and absorption work on NCO. Bondybey and English[10] observed fluorescence of matrix isolated NCO by pumping to the $A\,^2\Sigma^+$ $(0, 0^0, 0)$ state. The resulting fluorescence to the $X\,^2\Pi$ $(1, 0^1, 0)$ state occurs between 21 300–21 600 cm^{-1}, a range encompassing the 4658 Å laser excitation line. Additional confirmation that the 4658 Å laser line pumps to the $A\,^2\Sigma^+$ $(0, 0^0, 0)$ vibrational state comes from experimental absorption results combined with determinations of the $X\,^2\Pi$ $(1, 0^1, 0)$ energy. Absorption studies[5,6] of gas phase NCO show that the $A\,^2\Sigma^+\,(0, 0^0, 0) - X\,^2\Pi\,(0, 0^1, 0)$ transition lies in the frequency region 22 700–22 900 cm^{-1}. Combining this result with the average of three measurements of the $X\,^2\Pi$ $(1, 0^1, 0)$ energy level[9,10,12] 1274 cm^{-1}, indicates that the 4658 Å line falls in the right region for $A\,^2\Sigma^+\,(0, 0^0, 0) - X\,^2\Pi\,(1, 0^1, 0)$ excitation of NCO. None of the other laser lines overlap such a low-lying vibrational band so well, explaining the stronger fluorescence observed upon pumping with the 4658 Å line.

A scan of the fluorescence from the 4658 Å pump line using the 1 m monochromator at 0.60 Å FWHM resolution is shown in Fig. 5. The top trace is flame emission resulting primarily from the CH A–X (0, 0) P branch. The lower trace is the LEF spectrum. The spectra are of similar intensity, as shown, demonstrating the necessity for subtracting the flame emission. Seven bandheads from two vibrational bands previously observed in absorption experiments on the NCO $A-X$ system[5,6] may be readily identified in the fluorescence spectrum. Thus, the previous tentative assignment to NCO is confirmed. In addition, eight prominent lines are observed at regularly spaced intervals of about

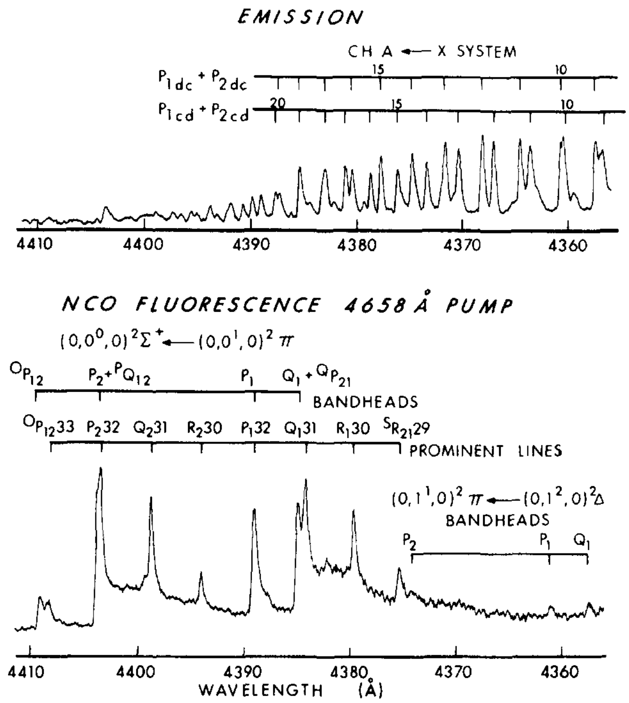

FIG. 5. Flame emission and LEF spectrum of NCO using the 4658 Å laser line. The spectra were taken at a resolution of 0.60 Å FWHM. Top trace: Flame emission arising mainly from the CH $A \leftarrow X$ system. Some weaker bandheads of NCO are also visible. Bottom trace: LEF spectrum of NCO in the $\Delta v = 0$ region.

4.5 Å in the spectrum. Two of these lines are only resolved from the bandheads in scans at the highest resolution available (0.17 Å FWHM). They are slightly to the violet of the P_1 and P_2 bandheads in Fig. 5. This pattern of lines is an indication that the number density in a rotational state of $A\,^2\Sigma^+$ $(0, 0^0, 0)$ having quantum number $N' = 30$ or 31 is much larger than for any other rotational state. It is common in a flame environment for a rotational level directly pumped by an excitation source in an electronically excited molecule to retain a higher population than nearby levels. This is demonstrated by fluorescence scans on OH,[20,21] CH,[22] CN,[16,22] and by indirect evidence from an excitation scan on NH for which the detector was biased towards fluorescence from only a few rotational levels.[23] This phenomenon demonstrates that rotational energy transfer in the excited state is not sufficiently fast to redistribute molecules to a Boltzmann distribution before they are quenched to the ground state.[16,20,21]

Evidence that $N' = 31$ is the level pumped by the 4658 Å excitation line is given in Fig. 6. A section of the Q_2-branch region at 0.17 Å FWHM is shown.[24] Two argon discharge lines[25] at 4401.02 and 4400.09 Å (not shown) are very close to the prominent Q_2 line of Fig. 6 and were used for calibration purposes[26] to establish the prominent line as Q_231.

As a cross check on the identification of the prominent Q_2 branch line, the Q_1 and R_1 branch line positions were checked against nearby known CH line positions (see Fig. 5). For this purpose, CH line positions were obtained from the work of Moore and Broida.[27] All of

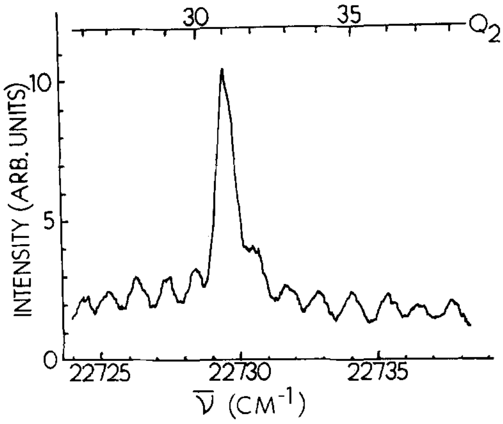

FIG. 6. Section from the Q_2 region of the LEF spectrum of NCO. The 4658 Å pump line was used. The spectrum was taken at the highest available resolution of 0.17 Å FWHM.

the NCO lines come from $N'=31$ if the assignment is correct, that is, the prominent Q_1 and R_1 branch lines are $Q_1 31$ and $R_1 30$. The CH $P_{cd}18$ and $P_{dc}18+P_{cd}19$ were used to calibrate the position of the Q_1 line while the CH $P_{cd}16$ and $P_{dc}16$ were used for the R_1 line.[28] The calibration indicated the Q_1 line position was most consistent with an assignment of $Q_1 31$. However, this line is near the Q_1 bandhead. Lines are so dense in this region that assignment to $Q_1 30$ or $Q_1 32$ could not be ruled out. This is not the case for the R_1 line as it is not near a bandhead. This line is firmly identified as $R_1 30$ in agreement with the identification of the $Q_2 31$ line. Therefore, all of the prominent lines of Fig. 5 must arise from $N'=31$. The prominent lines in Fig. 5 not identified by our calibrations were assigned on this basis. A full high resolution (0.17 Å FWHM) scan of the region in Fig. 5 along with calibration scans will be presented elsewhere.[28]

Efforts were made to identify the rotational branch pumped by the 4658 Å laser line and, hence, the (N'', J'') level from which pumping occurs. For this purpose, spectra were taken at 0.60 Å resolution in the region of the laser excitation line. An example is shown in Fig. 7. The strong peak at 4658 Å is due to scattered laser light. The peak drops to zero at line center because of saturation of the detection electronics. Three pairs of peaks positioned symmetrically about the pump line are grating ghosts and should be disregarded. The remainder of the spectrum is complicated by LEF from the C_2 Swan system.[15] Here the 4658 Å line excites in the (2, 1) band. Because the C_2 emission is much stronger than the NCO emission in this region we were able to compare the emission and fluorescence spectra ascribing peaks which occur in both to C_2. Grating ghosts were also eliminated from consideration. The remaining peaks (except for the laser line) are designated with arrows in Fig. 7.

The following observations may help interpret the spectrum of Fig. 7. Emission in the 4400 Å region results from the $A\,^2\Sigma^+\,(0,0^0,0)-X\,^2\Pi\,(0,0^1,0)$ vibrational band. The $A\,^2\Sigma^+(0,0^0,0)-X\,^2\Pi\,(1,0^1,0)$ band has the same overall symmetries of ground and excited states. Though no rotational analysis for the $X\,^2\Pi\,(1,0^1,0)$ state is available, one would expect its rotational constants to be nearly the same as those for the $X\,^2\Pi\,(0,0^1,0)$ state. Therefore, the rotational branch structure of these two vibrational bands should be quite similar. In particular, though minor differences might well occur, the relative spacings and intensities of the bandheads and prominent lines from $N'=31$ should be about the same for the two vibrational bands. Thus, if spectra for both bands are available on the same wavelength scale, an overlay of the two spectra should reveal similarities. (Note, of course, that the pumped transition will lie directly under the laser line.) We have overlaid transparencies of the spectra and compared them as described. This comparison leads to the best agreement when one assumes the Q_2 branch line is pumped. However, the assignment is not firm due to the C_2 and grating ghost interferences in Fig. 7.

Because of the expected similarities in rotational structure for the two vibrational bands of interest in the preceding paragraph, one can compute approximate positions of rotational lines in the $A\,^2\Sigma^+\,(0,0^0,0)-X\,^2\Pi\,(1,0^1,0)$ band by subtracting the energy of $X\,^2\Pi\,(1,0^1,0)$, 1274 cm^{-1}, from the energy for the corresponding rotational line in the $A\,^2\Sigma^+\,(0,0^0,0)-X\,^2\Pi\,(0,0^1,0)$ band. This has been done for all possible lines having $N'=31$. The result is shown in Table I. The $A\,^2\Sigma^+\,(0,0^0,0)-X\,^2\Pi\,(0,0^1,0)$ line positions were obtained from the absorption spectra.[5,6] The 4657.94 Å laser line[25] corresponds to an energy of 21 463 cm^{-1}. This clearly matches the estimated $Q_2 31$ position best in agreement with the overlay result. The slight discrepancy is not unreasonable considering the assumption of equal rotational constants for the two vibrational levels. However, the assignment of transition type as Q_2 is still not entirely conclusive. The error limits on measurements of the $X\,^2\Pi\,(1,0^1,0)$ energy are large enough that assignment of the pumping transition to the $P_2 32$ or $R_2 30$ cannot be ruled out. Though assignment to other than the Q_2 branch seems unlikely, a firm identification awaits further study.

The prominent lines in the spectrum in Fig. 5 also

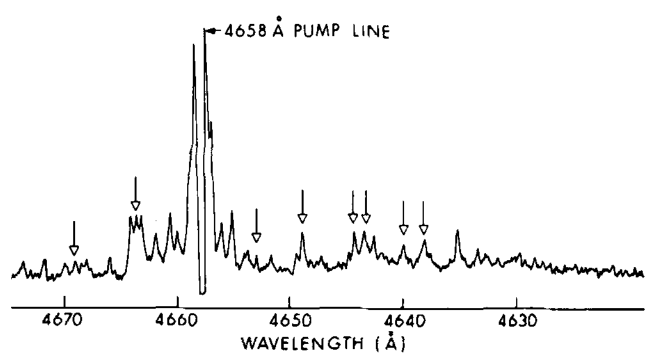

FIG. 7. LEF spectrum in the region of the 4658 Å pump line. The spectrum was taken at 0.60 Å FWHM resolution. The scattered light from the laser line dropped to zero due to saturation of the detection electronics. Three pairs of peaks placed symmetrically about the pump line were attributed to grating ghosts. Of the remaining peaks, those labeled with arrows are not present in the flame emission spectrum which, in this region, is mainly due to C_2.

TABLE I. Estimates of NCO $A \leftarrow X$ system line positions in 4658 Å region.[a]

Transition type	Known position in $(0,0^0,0) \leftarrow (0,0^1,0)$ (cm^{-1})	Estimated position $(0,0^0,0) \leftarrow (1,0^1,0)$ (cm^{-1})
${}^{O}P_{12}33$	22 679	21 405
$P_2 + {}^{P}Q_{12}32$	22 705	21 431
$Q_2 + {}^{Q}R_{12}31$	22 729	21 455
$R_2 30$	22 753	21 479
$P_1 32$	22 779	21 505
$Q_1 + {}^{Q}P_{21}31$	22 804	21 530
$R_1 + {}^{R}Q_{21}30$	22 829	21 555
${}^{S}R_{21}29$	22 852	21 578

[a]Known line positions were obtained from Refs. 5 and 6. Estimated line positions were obtained by subtracting the measured $X\,^2\Pi$ $(1, 0^1, 0)$ vibrational energy from the known positions as described in the text. The argon 4658 Å laser line corresponds to an energy of 21 463 cm^{-1}.

yield information about energy transfer in the excited NCO. As shown, the $Q_1 31$ and $Q_2 31$ intensities are nearly equal. Since one would expect nearly equal rotational line strengths for these transitions, these intensities indicate approximately equal densities in the F_1 and F_2 spin components for $N' = 31$, in contrast to observations made for the $A\,^2\Sigma^+$ state of OH in a flame.[21] These equal populations may arise either by excitation to one spin state followed by rapid spin state redistribution with retention of N' identity, or by equal pumping of two spin states via overlap of main and satellite branch transitions. A calculation of the excited state spin splitting using the spin-rotation constant of Ref. 6 yields $F_1 31 - F_2 31 = 0.016 \pm 0.005$ cm^{-1}. Since the Doppler width at the measured flame temperature of 2500 K is about 0.13 cm^{-1}, the main branch and satellite transitions are almost completely overlapped under these conditions. If pumping occurs via the P_2 branch and its satellite, both having similar transition strength,[6] then the two spin states will be equally populated by laser excitation. The other two possibilities for the pumping transition, however, favor collisional spin-state relaxation. Of these, the R_2 branch has no satellite and only one spin state can be pumped directly. As discussed earlier, it is most probable pumping occurs in the Q_2 branch where the strength of the main branch and satellite transitions differ by a factor of about 3. Therefore, the interpretation of spin-state relaxation is favored.

In scans of fluorescence from $A\,^2\Sigma^+$ $(0, 0^0, 0)$, besides the bands in the 4400 and 4658 Å region, Bondybey and English[10] also observed weaker emissions near 4485 and 4820 Å. These were attributed to emission to $X\,^2\Sigma^+$ $(0, 1^0, 0)$ and $X\,^2\Pi$ $(0, 0^1, 1)$, respectively. Corrections for detection system sensitivity versus wavelength were not made in their study nor in the present work, but the wavelength range scanned is small enough that the sensitivity is not expected to change drastically. (In particular, sensitivities for the PMTs used in the two studies change less than 15% over the region of interest). In the earlier study,[10] an unknown gain change was made between 4400 and 4485 Å. We have measured the intensity ratio for emission to $X\,^2\Pi$ $(0, 0^1, 0)$ and $X\,^2\Sigma^+$ $(0, 1^0, 0)$. Combining this with the earlier ratios for the three hot band intensities leads to an estimate of the intensity ratio between the two strongest bands. The resulting intensity ratio for $X\,^2\Pi$ $(0, 0^0, 0)$ to $X\,^2\Pi$ $(1, 0^1, 0)$ is about 2.8 : 1.[30] Emission to $X\,^2\Pi$ $(0, 0^1, 1)$ could not be found using the 1 m monochromator. This may be due to two factors. First, the emission may be too broad to be seen easily at high resolution. Second, the laser power and performance were deteriorating in the late part of this study when the most diligent attempts to find the band were made. However, a very weak and rather broad doublet was observed with the 25 cm monochromator-OMA system which could be attributed to this band. Though C_2 fluorescence interferes with exact measurements in the 4658 Å region, the intensity ratios for the three hot bands are at least in qualitative agreement with Ref. 10.

One fluorescence spectrum from those with broad spectral envelopes shown in Fig. 4 was selected for further study. The fluorescence intensity from the 4765 Å pump line was the strongest, about 0.2 times that from the 4658 Å line. A spectrum at 0.60 Å FWHM resolution taken with the 1 m monochromator is shown in Fig. 8. The spectrum is noisier than for that from 4658 Å (Fig. 5) due to the lower signal intensity. Nonetheless, the same seven bandheads as seen with the 4658 Å laser line may still be readily identified. In addition, several other bandheads and/or peaks at shorter wavelengths are present in Fig. 8. It is readily seen from Ref. 10 that these emissions do not arise from the $A\,^2\Sigma^+$ $(0, 0^0, 0)$ level. They may arise from excitation to some high vibrational level followed by vibrational relaxation populating a number of lower levels. Alternatively, the laser line could excite high-lying rotational levels from several vibrational levels in the ground state. Thus, the excitation line could populate more than one vibrational level in the A state resulting in a rather complex spectrum. Or, some combination of these two effects may take place. If significant vibrational relaxation does occur, it would seem to indicate that H_2O, CO_2, H_2, or CO (major species present under rich flame conditions) must be the collision partner since Sullivan *et al.*[12] have found that vibrational relaxation of $A\,^2\Sigma^+$ NCO by N_2 and O_2 is very slow. The doublet observed at about 4371 Å in Fig. 8 is rather intriguing. The sharpness of these peaks, similar in width to the prominent lines of Fig. 5, suggests that perhaps one or both of them are due to emission from an initially pumped N' level. Higher resolution scans would be necessary to evaluate this possibility. We have not pursued this type of study at present.

B. NCO density in the flame

The NCO fluorescence may be readily used to map out relative densities in the flame. This was done using the 4658 Å excitation line since this excitation is the best understood. Also, the line excites the $A\,^2\Sigma^+$ $(0, 0^0, 0)$ level so that vibrational transfer to lower levels will not complicate data analysis. The technique is explained in this section.

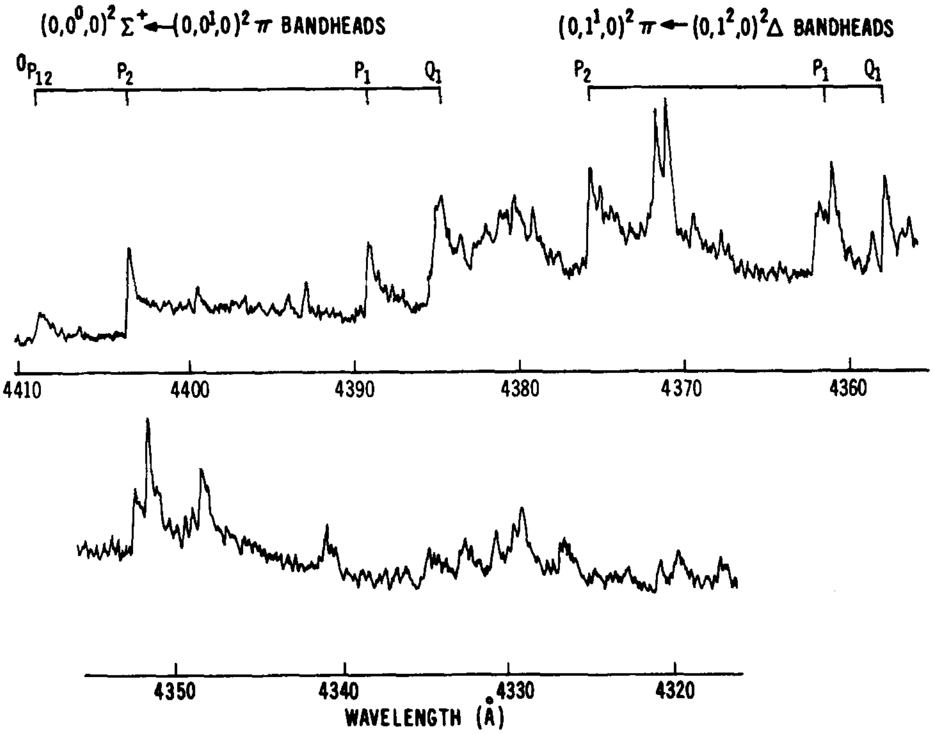

FIG. 8. LEF spectrum of NCO using the 4765 Å laser line. The spectrum was taken at 0.60 Å FWHM resolution.

Two basic assumptions must be made in order to make relative density measurements. First, one must assume the relative quenching rate is nearly constant throughout all positions of interest in the flame. At first glance, this assumption seems unreasonable for the flame front because the composition and temperature undergo drastic changes in that region. However, several recent studies indicate quenching rates are nearly constant in flame fronts, at least for OH.[23,31,32] As will be seen shortly, the temperature is fairly constant over much of the region of interest. Also, one typically finds for premixed flames that the major species composition approximates that in the burnt gases very early in the flame front. Therefore, the assumption of constant quenching rates is not unreasonable. The second basic assumption is that the X state of NCO is in thermal equilibrium at the flame temperature. One then calculates the relative density using the familiar Boltzmann equation. These assumptions lead to the very simple proportionality

$$\eta \propto F\, Q/(2J''+1)\exp(-E_{N'',J''}/kT)\ , \qquad (1)$$

where η is the density of NCO, F the fluorescence intensity, Q the molecular partition function, J'' is the angular momentum quantum number for the ground state, and $E_{N'',J''}$ is the energy of the ground rotational state. For the present results we assumed the 4658 Å line pumps the $Q_2 31$ transition for which the ground state is $N''=31$, $J''=30.5$. However, even if the assignment of rotational branch for the pumping transition is incorrect, the factors in Eq. (1) still lead to the same relative density profiles. However, the estimate of absolute density, to appear later, would be affected. If the R_2 or P_2 transition is actually pumped at 4658 Å, our estimate of the rotational line strength is about a factor of 2 too high so that the calculated density would be a corresponding factor too low. $E_{N'',J''}$ in Eq. (1) was estimated by using the measured[9,10,12] $X\,^2\Pi$ $(1, 0^1, 0)$ energy of 1274 cm^{-1} and assuming rotational constants are nearly equal in the $X\,^2\Pi$ $(0, 0^1, 0)$ and $(1, 0^1, 0)$ states. The spin-orbit splitting[5,6] of ~98 cm^{-1} in $X\,^2\Pi$ was also considered.

The relative fluorescence intensity profiles were measured using the 25 cm monochromator-OMA system. The strong fluorescence for the entire band system between 4300 and 4425 Å was integrated to yield the intensities versus burner position. Temperature measurements were made using the spontaneous Raman signal from the Stokes rotational-vibrational Q branch of N_2. These Raman spectra were fitted using a multiparameter least squares computer program developed to extract temperature and N_2 concentration from the data. The standard deviation in flame temperatures is about 1%. The Raman methods are discussed in more detail in Ref. 13. The resulting temperature and relative density profiles are shown in Fig. 9. The adiabatic flame temperature, calculated using the NASA–Lewis thermodynamic equilibrium code of Svehla and McBride,[33] is also indicated in the figure. Note that the measured peak temperature and adiabatic flame temperature are equal within experimental error, indicating minimal heat losses to the burner. The zero point on the relative position scale in Fig. 9 corresponds to the top of the burner body (see Fig. 1). The minimum distance between the top of the knife edges and the top of the burner body, where the measurements were taken, is 2.50 ± 0.25 mm. The steep concentration and temperature gradients at about 1.0–1.5 mm indicate the position of the leading edge of the flame reaction zone. Therefore, the reaction zone must extend about 1.0–1.5 mm below the top of the knife edges under our flow

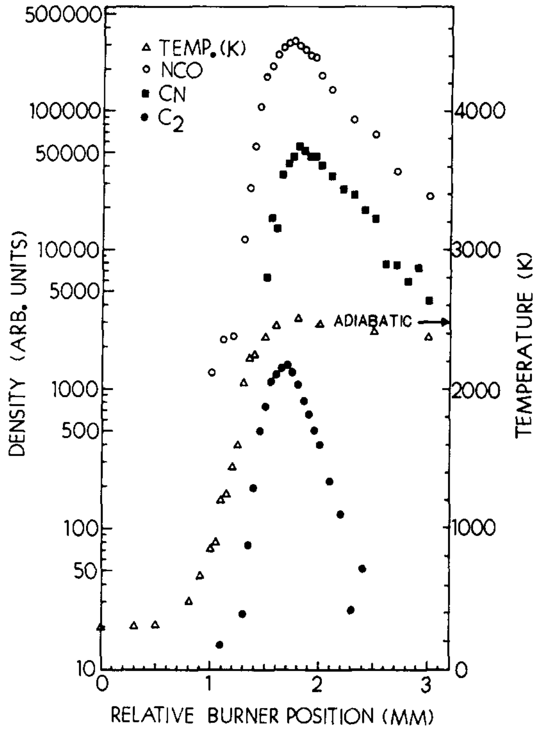

FIG. 9. Measured temperature and relative density profiles of NCO, CN, and $a\,^3\Pi_u$ C_2 in a slightly rich CH_4/N_2O flame. The calculated adiabatic flame temperature is also indicated. Relative densities may not be compared between compounds in this figure because curves for the individual compounds were only plotted with large separations for ease in visualization. Estimates of the absolute peak densities are given in the text.

conditions. (This agrees reasonably well with a visual inspection of the luminous flame zone position.)

Besides the NCO and temperature profiles, relative $a\,^3\Pi_u$ C_2 and $X\,^2\Pi$ CN profiles measured at the same time[15] are shown for comparison in Fig. 9. The density profiles are almost indistinguishable from the relative fluorescence intensity profiles (not shown), indicating the correction in Eq. (1) is small. It should be noted that the relative concentration profiles are only meaningful for individual compounds versus position; i.e., the absolute peak concentrations of the three compounds are not accurately known. Figure 9 shows that the C_2, CN, and NCO concentrations all decay rapidly outside the reaction zone of the flame.

As discussed in Ref. 15, a very rough estimate of the absolute peak densities in Fig. 9 may be made using three major assumptions. Briefly, one assumes: (1) the laser line is Doppler broadened at about room temperature,[34] (2) the molecular transition is Doppler broadened at the flame temperature of about 2500 K, and (3) the quenching rate of excited molecular species is about 1×10^9 s^{-1}, a typical value for atmospheric pressure flames.[35] Furthermore, measurements of NCO quenching rates by O_2 and N_2,[12] corrected to our temperature and pressure, indicate 1×10^9 s^{-1} is a reasonable estimate to select. The calculation also requires some knowledge of the overlap of the laser pump line and the molecular transition. Data was available to estimate this quantity for C_2 and CN, but of course not for NCO since exact line positions are unknown. Therefore, the calculation for NCO assumed perfect overlap. Thus, only a lower limit for the density was computed. Finally, the fluorescence intensity was calibrated against the Raman N_2 signal from room air using the same laser lines as for fluorescence excitation. Calibration in this manner has two advantages in that it obviates the need for an absolute laser power or a sampling volume measurement. Using estimated overlap for C_2 and CN leads to peak densities of 2×10^{13} and 3×10^{14} cm^{-3}, respectively.[15] Spectroscopic data used for these estimates is discussed in Ref. 15. For NCO, the further necessary spectral data is the relative intensity of vibrational bands associated with $A\,^2\Sigma^+$ (0, 0^0, 0) and the radiative lifetime of this state. These may then be used to calculate Einstein coefficients. The estimated relative vibrational band intensities were obtained as discussed in the previous section. The fluorescence lifetime used was 400 ns obtained from gas phase measurements.[11,12] The lower limit for NCO density thus calculated is 3×10^{14} cm^{-3}. Due to the various assumptions made in the absolute density calculations, it is difficult to place error limits on these quantities. The major source of random error in the calculated densities is in the spectral overlap because the densities are quite sensitive to these quantities. Of course, the lower limit for NCO does not depend on this quantity at all. Most probably the largest source of systematic error is in the assumed quenching rate of 1×10^9 s^{-1} which is probably only good to within about a factor of 5. The densities are, therefore, believed to be good to within factors of about 10 for CN, 20 for $a\,^3\Pi_u$ C_2, and 5 for the lower limit for NCO. These estimates should be useful in determining whether chemistry of these trace species must be considered in CH_4/N_2O flame models.

Attempts were made to find C_2, CN, and NCO in a slightly rich CH_4/air flame (exact composition unknown). The sensitivity limits were for densities about a factor of 100 lower than in the CH_4/N_2O flame. Fluorescence was found for C_2, but not for CN or NCO. This result indicates a probable difference in the nitrogen chemistry for the two flames. Earlier studies of OH and, in particular, NH concentrations in the stoichiometric flames led to the same conclusion.[23] This should not be extremely surprising because the N–N bond strength in N_2 is much stronger than in N_2O making N_2 more chemically inert. We have not attempted to analyze details of the chemistry at present.

IV. CONCLUSIONS

Laser excited fluorescence from the $A-X$ system of NCO has been identified in a rich atmospheric pressure CH_4/N_2O flame using an argon laser pump source. LEF was obtained for all nine available laser lines ranging from 4545–5145 Å. The hot flame source of NCO aids in the pumping scheme since all of the available laser lines must pump vibrational hot bands of the NCO to the red of the main 4400 Å band. The 4658 Å laser line appears to be by far the most useful of the available lines for diagnostic purposes. This line pumps in the $A\,^2\Sigma^+$ (0, 0^0, 0)$-X\,^2\Pi$ (1, 0^1, 0) band. It appears that this is why the LEF is most intense for this pump line. NCO is pumped to the $N'=31$ excited level by the 4658 Å line. However, the rotational branch of the pumping transition could not be firmly established. At present, the $Q_2 31$ appears to be the most likely candidate.

The 4658 Å pump line was used to measure accurate relative density profiles in the CH_4/N_2O flame. In addition, a lower limit for the absolute number density of $\sim 3\times10^{14}$ cm^{-3} was estimated using the available spectroscopic data and an assumed quenching rate. The argon laser source has proven to be quite useful for flame measurements of NCO. It should thus be useful for other hot sources of NCO in which cw measurements are desired.

ACKNOWLEDGMENTS

The authors gratefully acknowledge the help of Mr. Calvin E. Weaver in construction of detection system electronics. Also, we would like to thank Dr. Vladimir E. Bondybey for sending us copies of original spectral data used in Ref. 10.

[1](a) G. B. Debrow, J. M. Goodings, and D. K. Bohme, Combust. Flame **39**, 1 (1980). (b) C. Morley, 18th Symposium (International) on Combustion (The Combustion Institute, Pittsburgh, PA, 1981), p. 23. (c) Y. H. Song, D. W. Blair, V. J. Siminski, and W. Bartok, *ibid*. p. 53, and references therein.

[2](a) R. A. Beyer, BRL Memorandum Report No. ARBRL-MR-02816, A054328 (1978). (b) C. U. Morgan and R. A. Beyer, 15th JANNAF Combustion Meeting, Newport, R.I., Sept. 1978.

[3]R. A. Fifer and H. E. Holmes, J. Phys. Chem. (to be published).

[4]R. Holland, D. W. G. Style, R. N. Dixon, and D. A. Ramsay, Nature (London) **182**, 336 (1958).

[5]R. N. Dixon, Phil. Trans. R. Soc. London **252**, 165 (1960).

[6]P. S. H. Bolman, J. M. Brown, A. Carrington, I. Kopp, and D. A. Ramsay, Proc. R. Soc. London Ser. A **343**, 17 (1975).

[7]R. N. Dixon, Can. J. Phys. **38**, 10 (1960).

[8]H. Okabe, J. Chem. Phys. **53**, 3507 (1970).

[9]D. E. Milligan and M. E. Jacox, J. Chem. Phys. **47**, 5157 (1967).

[10]V. E. Bondybey and J. H. English, J. Chem. Phys. **67**, 2868 (1977).

[11]H. Reisler, M. Mangir, and C. Wittig, Chem. Phys. **47**, 49 (1980).

[12](a) B. J. Sullivan, G. P. Smith, D. R. Crosley, and G. Black, Eastern States Fall Technical Meeting of the Combustion Institute, Pittsburgh, PA, October 1981, paper 44. (b) B. J. Sullivan, G. P. Smith, and D. R. Crosley (to be published).

[13]J. A. Vanderhoff, R. A. Beyer, and A. J. Kotlar, BRL Report No. ARBRL-TR-02388, January 1982.

[14]J. A. Vanderhoff, R. A. Beyer, W. R. Anderson, and A. J. Kotlar, 36th Symposium on Molecular Spectroscopy, Columbus, Ohio, June 1981.

[15]J. A. Vanderhoff, R. A. Beyer, A. J. Kotlar, and W. R. Anderson, Combust. Flame (submitted).

[16]W. R. Anderson, A. J. Kotlar, and J. A. Vanderhoff (to be published).

[17]W. R. Anderson, J. A. Vanderhoff, A. J. Kotlar, L. J. Decker, and R. A. Beyer, Eastern States Fall Technical Meeting of the Combustion Institute, Pittsburgh, PA, October 1981, paper 47.

[18]Compare this to the overall flame molecular density of $\sim 3\times10^{18}$ cm^{-3} at 1 atm and the measured flame temperature 2500 K.

[19]R. A. Beyer and M. A. DeWilde, Rev. Sci. Instrum. **53**, 103 (1982).

[20]C. Chan and J. W. Daily, Appl. Opt. **19**, 1357 (1980).

[21]G. P. Smith and D. R. Crosley, 18th Symposium (International) on Combustion (The Combustion Institute, Pittsburgh, PA, 1981), p. 1511.

[22]A. C. Eckbreth, P. A. Bonczyk, and J. F. Verdieck, Report No. EPA-600/7-80-091, May 1980. Example spectra abstracted from this report may be found in: A. C. Eckbreth in *Laser Probes for Combustion Chemistry*, edited by D. R. Crosley (American Chemical Society Symposium Series 134, Washington, D.C., 1980), p. 271; J. F. Verdieck and P. A. Bonczyk, 18th Symposium (International) on Combustion (The Combustion Institute, Pittsburgh, PA., 1981), p. 1559.

[23]W. R. Anderson, L. J. Decker, and A. J. Kotlar, Combust. Flame. (to be published).

[24]At first glance the larger size of the $Q_2 32$ compared to the $Q_2 30$ in Fig. 6 suggests preferential rotational up transfer, which seems unreasonable. The larger size of $Q_2 32$ is probably due to overlap with the $R_2 16$. The laser linewidth is much too narrow to pump $N'=31$ and 32, simultaneously.

[25]Atomic line positions were obtained from G. R. Harrison, *Massachusetts Institute of Technology Wavelength Tables*, (M.I.T., Cambridge, Mass., 1969).

[26]It was discovered that the monochromator scan was not quite linear over long wavelength regions. The spectra in Figs. 5, 7, and 8 were scanned from longer to shorter wavelengths. Towards the shorter wavelengths the scans are only good to within about ± 0.5 Å. Therefore, high resolution scans were calibrated using known line positions of argon and CH emission. The calibration lines were chosen so that only short wavelength scans were required.

[27]C. E. Moore and H. P. Broida, J. Res. Natl. Bur. Stand. Sect. A **63**, 19 (1959).

[28]In the text, F-number subscripts for CH transitions are dropped for convenience since spin-orbit components were overlapped even at our highest available resolution.

[29]W. R. Anderson, J. A. Vanderhoff, A. J. Kotlar, M. A. DeWilde, and R. A. Beyer, BRL Report (to be published).

[30]In a private communication, V. E. Bondybey informed us that though exact information was lost, the approximate gain change should lead to an intensity ratio of about 2 or 3 : 1, in good agreement with our result. Approximate intensity ratios for the other two bands may be derived from the fluorescence scan in Ref. 10. The results are also in reasonable agreement with preliminary results of a more careful determination to appear in Ref. 12(b).

[31]J. H. Bechtel and R. E. Teets, Appl. Opt. **18**, 4138 (1979).

[32]M. J. Cottereau and D. Stepowski, in *Laser Probes for Combustion Chemistry*, edited by D. R. Crosley (American Chemical Society Symposium Series 134, Washington, D.C., 1980), p. 131.

[33]R. A. Svehla and B. J. McBride, NASA TN D-7056, 1973 (1981 program version).

[34]Actually the laser line shape probably consists of about 20–30 cavity modes within the 0.04 cm^{-1} Doppler width.

[35]A similar assumption is made in D. R. Crosley, Opt. Eng. **20**, 511 (1981).